Smart Structures and Systems, *Vol. 21, No. 4 (2018) 407-420*
DOI: https://doi.org/10.12989/sss.2018.21.4.407

A multitype sensor placement method for the modal estimation of structure

Xue-Yang Pei[1a], Ting-Hua Yi[*1] and Hong-Nan Li[1,2b]

[1]*School of Civil Engineering, Dalian University of Technology, Dalian 116023, China*
[2]*School of Civil Engineering, Shenyang Jianzhu University, Shenyang 110168, China*

(Received October 4, 2017, Revised March 11, 2018, Accepted March 12, 2018)

Abstract. In structural health monitoring, it is meaningful to comprehensively utilize accelerometers and strain gauges to obtain the modal information of a structure. In this paper, a modal estimation theory is proposed, in which the displacement modes of the locations without accelerometers can be estimated by the strain modes of selected strain gauge measurements. A two-stage sensor placement method, in which strain gauges are placed together with triaxial accelerometers to obtain more structural displacement mode information, is proposed. In stage one, the initial accelerometer locations are determined through the combined use of the modal assurance criterion and the redundancy information. Due to various practical factors, however, accelerometers cannot be placed at some of the initial accelerometer locations; the displacement mode information of these locations are still in need and the locations without accelerometers are defined as estimated locations. In stage two, the displacement modes of the estimated locations are estimated based on the strain modes of the strain gauge locations, and the quality of the estimation is seen as a criterion to guide the selection of the strain gauge locations. Instead of simply placing a strain gauge at the midpoint of each beam element, the influence of different candidate strain gauge positions on the estimation of displacement modes is also studied. Finally, the modal assurance criterion is utilized to evaluate the performance of the obtained multitype sensor placement. A bridge benchmark structure is used for a numerical investigation to demonstrate the effectiveness of the proposed multitype sensor placement method.

Keywords: optimal sensor placement; triaxial accelerometer; strain gauge; estimated locations; candidate strain gauge locations; modal estimation

1. Introduction

Sensor placement often plays a significant role in a structural health monitoring (SHM) system because the functionality of the SHM system is directly affected by the quantity and quality of the measured data (Yi *et al.* 2012a, Huang *et al*. 2017, Li and Hao 2016). The modal characteristics obtained from the measured data are crucial for obtaining the actual condition of the structure, which can be used to update the finite element (FE) model and perform damage detection (Worden and Burrows 2001, Chang and Pakzad 2014, Li *et al.* 2017). Generally, the higher the number of sensors placed on a structure is, the more structural modal information is obtained. However, it is neither economical nor practical to use a large number of sensors in a SHM system. Thus, instead of simply adding more sensors to obtain more structural response data, an optimal sensor placement (OSP) method is needed using limited sensors to obtain as much structural modal information as possible.

In previous studies, many OSP methods based on modal identification have been proposed, in which the single type of sensors (accelerometer) are often used. Some studies used the matrix analysis to solve the OSP problems, in which the modal expansion form of the measured data is usually used. The effective influence (EfI) method (Kammer 1991, Kammer and Tinker 2004) used the Fisher information matrix to select sensor locations according to the norm value. The driving point residue (DPR) method (Papadopoulos and Ephrahim 1998) was proposed to avoid selecting sensor locations with low energy, and the kinetic energy (KE) method (Heo *et al.* 1997) was proposed to take the mass matrix into account to use the KE matrix instead of the Fisher matrix; the connection between the EfI method and KE method was analyzed by Li *et al.* (2007). Some studies used the statistical analysis to solve the modal identification based OSP problems, in which the probability density of the estimated parameter was often used. Udwadia (1994) proposed a rational statistical-based theory of sensor placement for parameter estimation; it uses a suitable norm of the Fisher matrix to guarantee the quality of the estimation result. An entropy-based OSP method, which minimizes the information entropy of estimated parameters to select the best sensor locations for structural model updating, was proposed by Papadimitriou *et al.* (2000). Further research that considers the effect of the correlation of prediction error on the sensor selection was also

*Corresponding author, Professor
E-mail: yth@dlut.edu.cn
[a] Ph.D. Student
E-mail: xypei@mail.dlut.edu.cn
[b] Professor
E-mail: hnli@dlut.edu.cn

ISSN: 1738-1584 (Print), 1738-1991 (Online)

developed (Paradimitriou and Lombaert 2012). The displacement modes provides a visual reflection of the structural dynamic characteristics and plays a very important role in the structural modal analysis (i.e., FE model updating, structure damage detection). In practice, mode shapes are only useful when the obtained mode shapes can be easily distinguished from each other (Penny *et al.* 1994). Then, a criterion that uses the correlation of the selected mode shapes to evaluate the sensor placement, known as the modal assurance criterion (MAC), was proposed by Carne and Dohrmann (1995). An improvement to the MAC method, which considered the case of the optimal selection of a sensor location on a high-rise building using a simplified finite element model, was proposed by Yi *et al.* (2012b). According to the MAC, some intelligence algorithms can be used to obtain a more accurate accelerometer placement (Yi *et al.* 2015a, b).

In practice, strain gauges and accelerometers are often used together in the SHM system. Some OSP method comprehensively utilizing multi types of sensors were proposed, in which strain gauges and accelerometers are placed together instead of placed separately. Yuen *et al.* (2015) proposed an efficient Bayesian sensor placement method combining the Bayesian spectral density approach and the information entropy to obtain a heuristic sequential optimization algorithm, in which the minimum uncertainty of the estimated structural parameter is guaranteed. Zhang *et al.* (2014) proposed an integrated optimal placement method of displacement transducers and strain gauges for response reconstruction, in which the reconstruction error is used to evaluate the sensor selection. Furthermore, Zhang *et al.* (2016) used the Kalman filter to guide the sensor placement to obtain the best estimation of the responses at key locations, in which strain gauges, displacement sensors and acceleration sensors are placed together. The relationship between the strain mode and the displacement mode was proposed by Yam *et al.* (1996), thus a mode estimation method using the strain mode to estimate the displacement mode is theoretical possible. However, few existing studies regarding strain and acceleration sensor placement methods focused on modal estimation. It is meaningful to use strain gauges to obtain more displacement mode information of locations without accelerometers. The problem of acquiring data from the strain gauges and accelerometers can be solved by a polytypic and synchronous data acquisition device (Ren *et al.* 2016). In addition, in the existing OSP literature related to strain gauges (Yuen *et al.* 2015, Zhang *et al.* 2014, Zhang *et al.* 2016), the midpoints of each structural element along the longitudinal axis are often used as the candidate strain gauge positions without explanations. The influence of different candidate strain gauge positions on the estimation of displacement modes needs to be further studied.

This paper proposes a multitype sensor placement method using the strain gauges and triaxial accelerometers together to obtain structural displacement mode information. In this method, a modal estimation theory is proposed, in which the displacement modes of the estimated locations without accelerometers are estimated by the strain modes of the selected strain gauge locations. The initial accelerometer locations are selected by the MAC and the redundancy information to guarantee the distinguishability and small redundancies of the obtained displacement modes at the same time. The estimated locations are determined via comprehensive consideration of the selected performance criteria and the practical situation. The optimal strain gauge locations are selected according to the smallest trace value of the covariance matrix of the estimated displacement mode vector, which is used to represent the uncertainty of the estimation. In addition, candidate strain gauge positions are determined by the amount of contained displacement mode information, which can be calculated by utilizing the transformation matrix between the displacement mode and the strain mode. The remaining sections of the paper are organized as follows: Section 2 presents the theory formulation of the sensor placement method. In Section 3, a bridge benchmark structure is used to verify the effectiveness of the proposed method. Finally, conclusions are drawn in Section 4.

2. Theory formulation of the modal estimation method

In this proposed sensor placement method, strain gauges only measure the normal strains. In addition, triaxial accelerometers are used in this theory formulation to ensure that the problem of the placement of accelerometers with less axes can be resolved by using the proposed sensor placement method.

2.1 Selection of initial accelerometer locations

As mentioned before, when conducting a modal test, the mode shape data are only useful when the mode shapes can be distinguished from each other. Thus, the MAC method is used here to select the initial accelerometers. The MAC matrix can be expressed as

$$\mathbf{MAC}_{i,j} = \frac{\left(\boldsymbol{\Phi}_{*,i}^{T}\boldsymbol{\Phi}_{*,j}\right)^{2}}{\left(\boldsymbol{\Phi}_{*,i}^{T}\boldsymbol{\Phi}_{*,i}\right)\left(\boldsymbol{\Phi}_{*,j}^{T}\boldsymbol{\Phi}_{*,j}\right)} \tag{1}$$

where $\boldsymbol{\Phi}_{*,i}$ and $\boldsymbol{\Phi}_{*,j}$ are the ith and jth columns of the target mode shape matrix, respectively. Considering the application of triaxial accelerometers, each accelerometer location corresponds to three rows in the target mode shape matrix. Every time, only one accelerometer location that gets the smallest value of the maximum off-diagonal MAC term is added to the existing placement.

In the MAC method, before adding sensors, the triaxial effective influence (TEfI) method can be used to determine the first several initial locations

$$\mathbf{EfI}3_{i} = 1 - \det\left(\mathbf{I}_{3} - \boldsymbol{\Phi}_{3i}\left(\boldsymbol{\Phi}_{s}^{T}\boldsymbol{\Phi}_{s}\right)^{-1}\boldsymbol{\Phi}_{3i}^{T}\right) \tag{2}$$

where $\mathbf{EfI}3_{i}$ denotes the contribution of the ith triaxial accelerometer location to the linear independence of the target modal partitions, $\boldsymbol{\Phi}_{s}$ is the target mode shape

matrix, and Φ_{3i} represents the three rows of the mode shape matrix of the ith accelerometer location. The TEfI method starts from all candidate accelerometer locations; every time, only one accelerometer location with the smallest contribution is deleted until the target number is reached.

Considering the continuity of the mode shapes, when two sensors are placed too close to each other, they usually contain similar modal information (Stephan 2012). Here, the Frobenius norm is used to evaluate the similarity of mode shapes of different locations, and the redundancy coefficient is defined as

$$\mathbf{R}_{i,j} = 1 - \frac{\left\| \mathbf{\Phi}_{3i} - \mathbf{\Phi}_{3j} \right\|_F}{\left\| \mathbf{\Phi}_{3i} \right\|_F + \left\| \mathbf{\Phi}_{3j} \right\|_F} \tag{3}$$

where $\mathbf{R}_{i,j}$ is the redundancy coefficient between the mode shapes of the ith and the jth locations. When the value of $\mathbf{R}_{i,j}$ is close to one, the two corresponding locations share almost the same modal information. A redundancy threshold T can be set to evaluate the redundancy information between different accelerometer locations, and a smaller threshold value means that less redundancy information is contained at the selected locations. An appropriate redundancy threshold value needs to be determined according to the concrete sensor placement process.

Finally, the selection process of the initial accelerometer placement is as follows:

Step 1: Determine the FE model of the benchmark structure and use the nodes as the candidate accelerometer locations.

Step 2: Use the TEfI method to obtain the first k accelerometer locations.

Step 3: Choose a value of the redundancy threshold T.

Step 4: Calculate the redundancy coefficients between the selected locations and the remaining candidate locations; if one redundancy coefficient is larger than T, the corresponding location will be deleted from the candidate locations.

Step 5: Assume that one of the candidate accelerometer locations is added to the selected locations, then calculate the values of the maximum off-diagonal terms of the MAC. Among all the candidate locations, the location corresponding to the smallest value is selected to be added to the existing placement.

Step 6: If no candidate locations remain, go to the next step; otherwise, return to step 4.

Step 7: Choose the first m accelerometer locations as the initial placement under the redundancy threshold T.

Step 8: If smaller redundancy threshold values can be accepted, change the value of the redundancy threshold T and return to step 3; otherwise, go to the next step.

Step 9: Compare the accelerometer placements obtained from the different redundancy threshold values, then choose an appropriate redundancy threshold T; the initial accelerometer locations are determined at the same time.

2.2 Selection of estimated locations without accelerometers

Sometimes, after the initial accelerometer locations have been determined one by one by using the above algorithm according to the performance criteria, the number of accelerometers can be decreased due to various practical factors. Here, two situations are considered. One situation is the limited economic budget, in which several of the last added accelerometer locations need to be deleted in order from last to first because the initial accelerometer locations are selected using a one-by-one sequential algorithm. The other situation is that some of the initial accelerometer locations are not suitable to receive accelerometers; thus, several locations will be deleted from the initial locations. Instead of deleting the locations in order, these locations are randomly deleted according to the practical situation. Although some accelerometer locations are deleted from the initially selected accelerometer locations, the displacement mode information of these locations is still important to the structural analysis because these locations are selected based on the performance criteria. Finally, these deleted locations with important displacement mode information are defined as the estimated locations, and the displacement modes of these estimated locations can be estimated based on the strain modes obtained from the strain gauges.

2.3 Selection of strain gauge locations for modal estimation

The relationship between the strain mode and the displacement mode is derived based on the finite element method. In the FE model, each node has six degrees of freedoms, which consist of three translations and three rotations in three directions, respectively. Then, the linear dynamical equation of the FE model can be written as

$$\mathbf{M}\ddot{\boldsymbol{\delta}} + \mathbf{C}\dot{\boldsymbol{\delta}} + \mathbf{K}\boldsymbol{\delta} = \mathbf{f} \tag{4}$$

where $\mathbf{M}$, $\mathbf{C}$ and $\mathbf{K}$ are the mass, damping and stiffness matrixes of the system, respectively; $\mathbf{f}$ is the input vector, regarding which locations of the excitations have been considered; $\boldsymbol{\delta}$ is the nodal displacement vector of all nodes in the global coordinate system, and a dot over the vector represents the derivative with respect to time.

In the ith element of the FE model, the relationship between the strains and the nodal displacements in the local coordinate system is expressed as

$$\boldsymbol{\varepsilon}_i = \mathbf{B}_i \boldsymbol{\delta}_i^e \tag{5}$$

where $\boldsymbol{\varepsilon}_i$ is the strain vector of the candidate locations; $\boldsymbol{\delta}_i^e$ is the nodal displacement vector of the ith element in the local coordinate system; $\mathbf{B}_i$ is the transformation matrix between the strain vector and the local nodal displacement vector, the form of $\mathbf{B}_i$ is determined by the FE model of the structure and the candidate strain gauge locations.

In the whole FE model, the relationship between the strains and the nodal displacements in the global coordinate

system is expressed as

$$\boldsymbol{\varepsilon} = \tilde{\mathbf{B}}\boldsymbol{\delta} \tag{6}$$

where $\boldsymbol{\varepsilon}$ is the strain vector of strains of candidate locations in the whole FE model, which consists of the strain vectors in different elements; $\tilde{\mathbf{B}}$ is the transformation matrix between the strains and the global nodal displacement of all nodes, the form of $\tilde{\mathbf{B}}$ is determined by the FE model of the structure and the candidate strain gauge locations.

Taking the modal expansion of the displacement vector into account, the Eq. (6) can be further written as

$$\boldsymbol{\varepsilon} = \tilde{\mathbf{B}}\boldsymbol{\delta} = \tilde{\mathbf{B}}\boldsymbol{\Phi}\mathbf{q} = \boldsymbol{\Psi}\mathbf{q} \tag{7}$$

Thus, the relationship between the strain mode and the displacement mode is obtained as

$$\boldsymbol{\Psi} = \tilde{\mathbf{B}}\boldsymbol{\Phi} \tag{8}$$

where $\boldsymbol{\Psi}$ denotes the strain mode matrix of the candidate strain locations; $\boldsymbol{\Phi}$ denotes the displacement mode matrix of all nodes; $\mathbf{q}$ denotes the modal coordinates.

The mode shapes obtained from the measurements often differ from the actual structural system output and the prediction error usually occurs due to the measurement noise and the FE model deviation (Beck and Katafygiotis 1998, Shi *et al*. 2000). Thus, the Eq. (8) can be further written as

$$\boldsymbol{\Psi} = \tilde{\mathbf{B}}\boldsymbol{\Phi} + \mathbf{v} \tag{9}$$

where $\mathbf{v}$ is a error matrix in which the ith column $\mathbf{v}_{(i)}$ has zero mean and a covariance $Cov(\mathbf{v}_{(i)}) = \sigma_i \mathbf{I}$. In the Eq. (9), when the number of rows of the strain mode matrix is greater than or equal to the number of rows of the displacement mode matrix, the least squares estimation method can be used to estimate the displacement modes through the strain modes. As mentioned in the section 2.2, in the displacement mode shape matrix $\boldsymbol{\Phi}$, only the rows corresponding to the estimated locations need to be estimated. Then, the right side of Eq. (8) can be transformed into

$$\tilde{\mathbf{B}}\boldsymbol{\Phi} = \sum_{i=1}^{N_d} \tilde{\mathbf{B}}_{\mathrm{i}} \boldsymbol{\Phi}_{\mathrm{i}} \tag{10}$$

$$\tilde{\mathbf{B}}\boldsymbol{\Phi} = \tilde{\mathbf{B}}^{r}\boldsymbol{\Phi}^{r} + \tilde{\mathbf{B}}^{N_d - r}\boldsymbol{\Phi}^{N_d - r} \tag{11}$$

where N_d is the number of rows of the displacement mode matrix $\boldsymbol{\Phi}$; $\tilde{\mathbf{B}}_{\mathrm{i}}$ is the ith column of the transformation matrix $\tilde{\mathbf{B}}$; $\boldsymbol{\Phi}_{\mathrm{i}}$ is the ith row of the displacement mode matrix; r is the number of rows of the displacement modes that need to be estimated in the displacement mode matrix $\boldsymbol{\Phi}$; $\boldsymbol{\Phi}^{r}$ denotes the r rows of $\boldsymbol{\Phi}$ corresponding to the estimated locations; $\boldsymbol{\Phi}^{N_d - r}$ denotes the remaining $N_d - r$ rows of $\boldsymbol{\Phi}$; $\tilde{\mathbf{B}}^{r}$ denotes the r columns of $\tilde{\mathbf{B}}$ corresponding to the estimated locations; $\tilde{\mathbf{B}}^{N_d - r}$ denotes the remaining $N_d - r$ columns of $\tilde{\mathbf{B}}$.

The selection of strain gauges involves selecting some rows in the strain mode shape matrix of all the candidate strain gauge locations; Eq. (9) can be re-written as

$$\mathbf{P}\boldsymbol{\Psi} = \mathbf{P}\left(\tilde{\mathbf{B}}\boldsymbol{\Phi} + \mathbf{v}\right) \tag{12}$$

where $\mathbf{P}$ is a selection matrix that consists of only zeros and ones and the number of rows of $\mathbf{P}$ is equal to the number of selected strain gauges. Then, Eq. (12) can be further re-written as

$$\mathbf{P}\left(\boldsymbol{\Psi} - \tilde{\mathbf{B}}^{N_d - r}\boldsymbol{\Phi}^{N_d - r}\right) = \mathbf{P}\tilde{\mathbf{B}}^{r}\boldsymbol{\Phi}^{r} + \mathbf{P}\mathbf{v} \tag{13}$$

In Eq. (13), when the number of selected strain gauges is greater than or equal to the number of rows of the displacement mode matrix $\boldsymbol{\Phi}^{r}$, the least squares estimation of the displacement modes of estimated locations can be obtained

$$\hat{\boldsymbol{\Phi}}^{r} = \left(\tilde{\mathbf{B}}^{rT}\mathbf{P}^{T}\mathbf{P}\tilde{\mathbf{B}}^{r}\right)^{-1}\tilde{\mathbf{B}}^{rT}\mathbf{P}^{T}\mathbf{P}\left(\boldsymbol{\Psi} - \tilde{\mathbf{B}}^{N_d - r}\boldsymbol{\Phi}^{N_d - r}\right) \tag{14}$$

$$\hat{\boldsymbol{\Phi}}^{r}_{(i)} = \left(\tilde{\mathbf{B}}^{rT}\mathbf{P}^{T}\mathbf{P}\tilde{\mathbf{B}}^{r}\right)^{-1}\tilde{\mathbf{B}}^{rT}\mathbf{P}^{T}\mathbf{P}\left(\boldsymbol{\Psi}_{(i)} - \tilde{\mathbf{B}}^{N_d - r}\boldsymbol{\Phi}^{N_d - r}_{(i)}\right) \tag{15}$$

where $\hat{\boldsymbol{\Phi}}^{r}$ is the estimation of $\boldsymbol{\Phi}^{r}$; $\hat{\boldsymbol{\Phi}}^{r}_{(i)}$ is the ith column of the matrix $\hat{\boldsymbol{\Phi}}^{r}$; $\boldsymbol{\Psi}_{(i)}$ is the ith column of the matrix $\boldsymbol{\Psi}$; $\boldsymbol{\Phi}^{N_d - r}_{(i)}$ is the ith column of the matrix $\boldsymbol{\Phi}^{N_d - r}$, which is obtained from the FE model. It is noted that if the matrix $\tilde{\mathbf{B}}^{rT}\mathbf{P}^{T}\mathbf{P}\tilde{\mathbf{B}}^{r}$ is singular, $\left(\tilde{\mathbf{B}}^{rT}\mathbf{P}^{T}\mathbf{P}\tilde{\mathbf{B}}^{r}\right)^{-1}$ represents the pseudo-inverse of the matrix $\tilde{\mathbf{B}}^{rT}\mathbf{P}^{T}\mathbf{P}\tilde{\mathbf{B}}^{r}$. The covariance matrix of the estimation vector $\hat{\boldsymbol{\Phi}}^{r}_{(i)}$ is expressed as

$$Cov(\hat{\boldsymbol{\Phi}}^{r}_{(i)}) = \sigma_i^2(\tilde{\mathbf{B}}^{rT}\mathbf{P}^{T}\mathbf{P}\tilde{\mathbf{B}}^{r})^{-1} \tag{16}$$

Considering the situation in which the diagonal terms of $Cov(\hat{\boldsymbol{\Phi}}^{r}_{(i)})$ represent the error of the estimation in each location of the ith modes, the trace of the covariance matrix $Cov(\hat{\boldsymbol{\Phi}}^{r}_{(i)})$ is used to evaluate the estimation uncertainty

$$error\left(\hat{\boldsymbol{\Phi}}^{r}_{(i)}\right) = \sigma_i \mathrm{tr}\left(\sqrt{\left(\tilde{\mathbf{B}}^{rT}\mathbf{P}^{T}\mathbf{P}\tilde{\mathbf{B}}^{r}\right)^{-1}}\right) \tag{17}$$

where tr denotes the trace. The uncertainty of the estimation matrix $\hat{\boldsymbol{\Phi}}^{r}$ consists of the uncertainty of different columns of the matrix, which is expressed as

$$\begin{aligned} error\left(\hat{\boldsymbol{\Phi}}^{r}\right) &= \sum_{i=1}^{N_m} error\left(\hat{\boldsymbol{\Phi}}^{r}_{(i)}\right) \\ &= \sum_{i=1}^{N_m} \sigma_i \mathrm{tr}\left(\sqrt{\left(\tilde{\mathbf{B}}^{rT}\mathbf{P}^{T}\mathbf{P}\tilde{\mathbf{B}}^{r}\right)^{-1}}\right) \end{aligned} \tag{18}$$

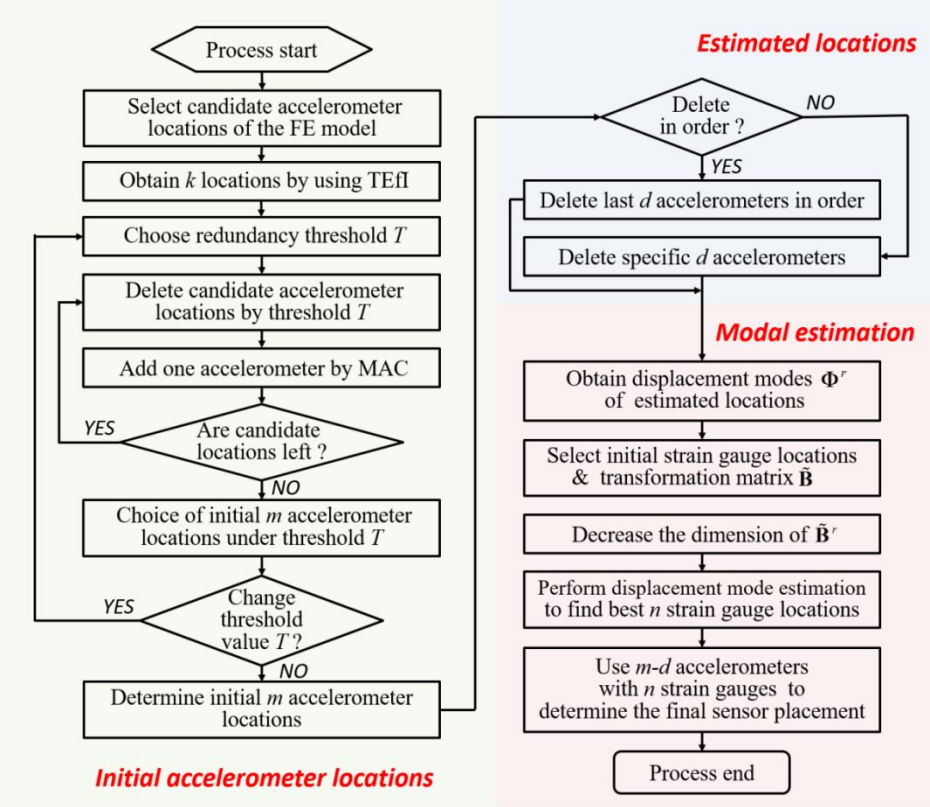

Fig. 1 Flowchart of the multitype sensor placement

where N_m is the number of mode orders. It can be seen from Eq. (18) that the estimation uncertainty of $\hat{\boldsymbol{\Phi}}^r$ is affected by the trace value, thus, Eq. (18) can be further re-written as

$$error\left(\hat{\boldsymbol{\Phi}}^r\right) \propto \mathrm{tr}\left(\sqrt{\left(\tilde{\mathbf{B}}^{rT}\mathbf{P}^T\mathbf{P}\tilde{\mathbf{B}}^r\right)^{-1}}\right) \tag{19}$$

Then, the evaluation of the estimated displacement mode matrix can be replaced by the evaluation of any column of the matrix, which reduces the computational effort. Considering the existence of the prediction error, the rows of $\tilde{\mathbf{B}}^r$ containing nothing but zeros can be deleted before calculating to reduce the dimension of $\tilde{\mathbf{B}}^r$, which can improve the quality of the displacement mode estimation. Finally, the best selection of the strain gauge locations is obtained from the selection matrix corresponding to the smallest value of estimation uncertainty.

The displacement mode estimation process is as follows:

Step 1: Determine the estimated displacement mode matrix $\boldsymbol{\Phi}^r$ in the Eq. (11) which is corresponding to the r estimated locations determined in the section 2.2.

Step 2: Determine the candidate strain gauge locations on each beam element of the structure, which is introduced detailedly in the section 3.2. Obtain the transformation matrix $\tilde{\mathbf{B}}$ in the Eq. (6) according to the FE model and the candidate strain gauge locations.

Step 3: Determine $\tilde{\mathbf{B}}^r$ according to the Eq. (11); delete the rows containing nothing but zeros.

Step 4: Use the Eq. (19) to evaluate the estimation error of the different strain gauge selections (different selection matrix $\mathbf{P}$); the smallest trace value corresponds to the best n strain gauge locations.

Step 5: Use the remaining $m-r$ accelerometers and selected n strain gauges to determine the final sensor placement.

2.4 Flowchart of the multitype sensor placement method

Fig. 1 shows the flowchart of the multitype sensor placement method, the process of which was introduced in the above sections.

3. Numerical studies

To demonstrate the effectiveness of the proposed multitype sensor placement method, a bridge benchmark structure (Catbas *et al.* 2008) is used for numerical investigation in this section, which was developed at the University of Central Florida (USA) to study the SHM techniques applied to medium-span bridges. The linear FEmodel of the bridge structure is built using SAP2000 Finite Element software, in which beam elements with 6 degrees of freedom at each node are preferred. Figs. 2 and 3

show the diagram and the FE model of the bridge benchmark structure, respectively. As shown in Fig. 3(a), the longitudinal girder members and the cross members of the FE model are subdivided into 11 and 7 elements, respectively. Thus, the FE model has 177 nodes and 181 elements in total, in which the 6 column elements are taken into account. Practically, for modal testing, excluding the 6 columns, sensors are often placed on the bridge deck, and the first 10 mode shapes obtained from the FE model are adopted here for sensor placement investigation. As shown in Fig. 3(b), 171 red nodes are considered as candidate triaxial accelerometer locations, and strain gauges are placed on 175 blue beam elements.

3.1 Selection of initial triaxial accelerometer locations

At the beginning, several accelerometer locations are selected according to the TEfI method. In the TEfI method, when performing the least squares estimation, the number of equations needs to be greater than or equal to the number of variables that need to be estimated.

(a) The bridge benchmark structure

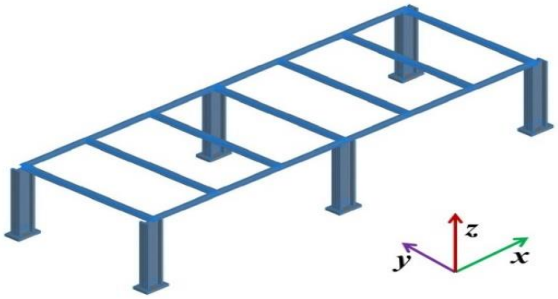

(b) Three-dimensional view

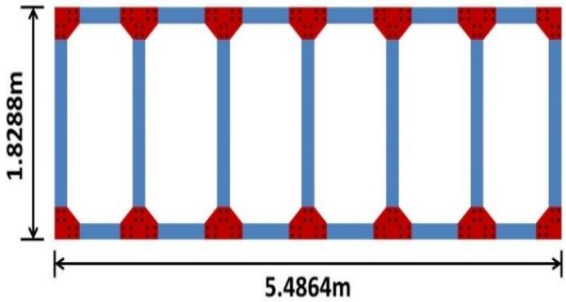

(c) Plan view with detailed size

Fig. 2 Diagram of the bridge benchmark structure

Thus, the number of accelerometer locations is determined to be 4. Then, more sensors can be added to the existing accelerometer placement one by one by comparing the value of the maximum off-diagonal term in the MAC matrix, with the concept of redundancy information also considered in every step. Here, five different redundancy threshold values, i.e., 0.8, 0.7, 0.6, 0.5 and 0.4, have been discussed in the accelerometer placement process, and an appropriate redundancy threshold T will be obtained after a concrete analysis.

Fig. 4 demonstrates the variation of the value of the maximum off-diagonal term in the MAC matrix with the number of added accelerometers, which increases from 1 to 15, under different redundancy threshold values. As shown in Fig. 4, the three curves corresponding to threshold values of 0.8, 0.7 and 0.6 are almost the same when the added sensor number is no more than five, which indicates that the redundancy coefficients between the first several added accelerometers are smaller than 0.6. Furthermore, the ends of the curves corresponding to the threshold values of 0.6 and 0.5 undergo an obvious increase, while the ends of the curves with redundancy threshold values of 0.8 and 0.7 decline smoothly. A close look at the added sensor number also shows that no more than thirteen sensors can be added when the threshold value is 0.6, no more than eight sensors can be added when the threshold value is 0.5 and only four sensors can be added when the threshold value is 0.4. The explanation for such a phenomenon is that the smaller a redundancy threshold T is set, the greater the number of accelerometer locations deleted from the candidate locations. When a redundancy threshold that is too small is set, the selected accelerometer locations cannot satisfy the MAC very well at the same time. As shown in Fig. 4, when the added sensor number is larger than 4, the curves with threshold values of 0.8, 0.7, 0.6 and 0.5 have no obvious decrease compared to the situation in which the added sensor number is smaller than 4.

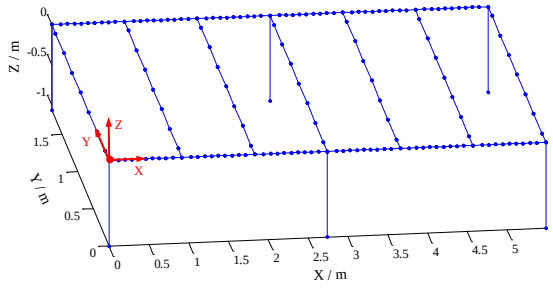

(a) Three-dimensional view

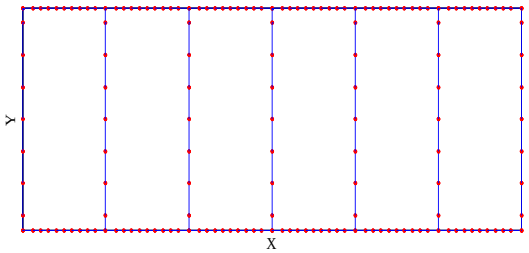

(b) Candidate accelerometer locations of the benchmark structure

Fig. 3 FE model of the benchmark structure

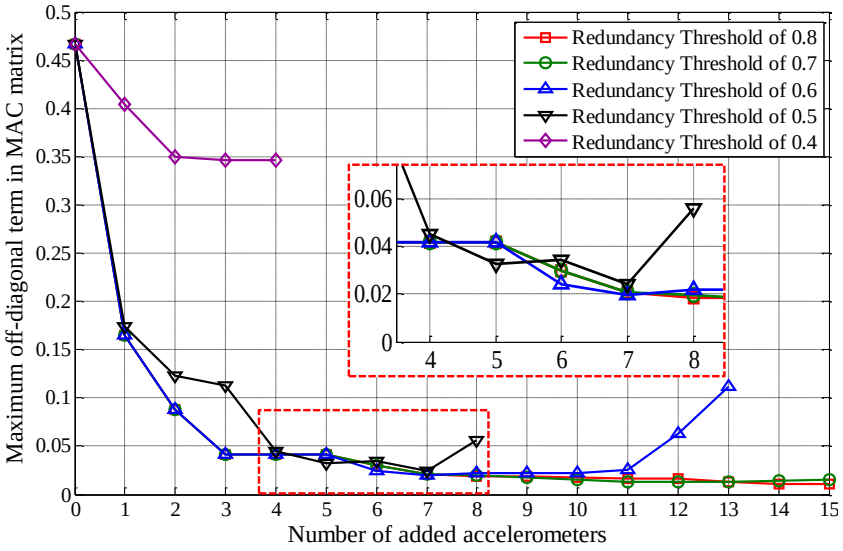

Fig. 4 Maximum off-diagonal term in MAC matrix under different redundancy thresholds

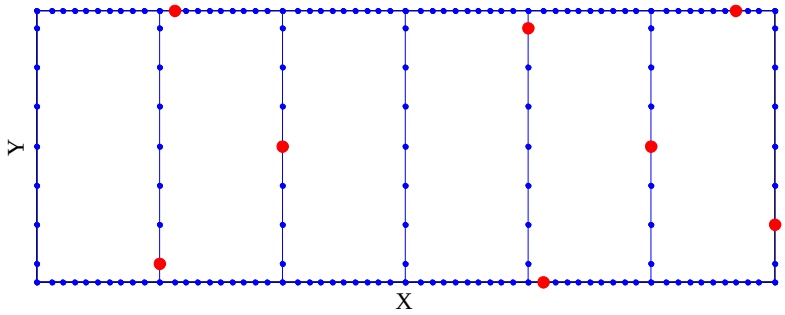

Fig. 5 Eight initial accelerometer locations for a redundancy threshold of 0.5

When the added sensor number is larger than 4, the maximum off-diagonal term in the MAC matrix for different threshold values of 0.8, 0.7, 0.6 and 0.5 are very similar. The value of the maximum off-diagonal term in the MAC matrix for a threshold value of 0.4 is too large. Furthermore, the maximum value of the redundancy coefficients of the four accelerometer locations selected by the TEfI method is 0.48. Considering the MAC and the redundancy information together, the redundancy threshold value chosen is 0.5, and the number of added accelerometers is determined to be 4. Finally, 8 accelerometer locations are selected as the initial accelerometer locations, and Fig. 5 shows the concrete locations of the 8 placed accelerometers, in which the red solid circles represent the selected accelerometer locations. In addition, if mode shape visualization is needed, more accelerometers can be added to the existing sensor placement, which is not discussed in this paper.

3.2 Determination of candidate strain gauge locations

In this benchmark model, all the beam members of the benchmark model have the same cross section as the S3×5.7 steel section at all locations except the joint connection regions, where the height of the joint connection cross section is little larger. Here, the Euler-Bernoulli theory, in which each beam element has two nodes and each node has six degrees of freedom, consisting of three translations and three rotations along three directions, is applied. In the local coordinate system, only the normal strains are measured; every normal strain is caused by axial force along the x direction, bending moments in the $x-y$ plane and bending moments in the $x-z$ plane. Then, in the ith beam element, the transformation matrix between the strain vector and the local nodal displacement vector is expressed as

$$\mathbf{B}_i = \mathbf{B}_{ix} + \mathbf{B}_{ix-y} + \mathbf{B}_{ix-z} \tag{20}$$

where $\mathbf{B}_i$ is the transformation matrix between the strain vector and the local nodal displacement vector; $\mathbf{B}_{ix}$ denotes the transformation matrix contributed by the axial force, and $\mathbf{B}_{ix-y}$ and $\mathbf{B}_{ix-z}$ are the transformation matrixes contributed by the bending moments in the $x-y$ plane and $x-z$ plane, respectively. Then, in the ith beam element, the relationship between strain modes and

local displacement modes is obtained as

$$\boldsymbol{\Psi}_i = \mathbf{B}_i \boldsymbol{\Phi}_i^e \tag{21}$$

where $\boldsymbol{\Psi}_i$ is the strain mode vector of candidate locations in the ith beam element and $\boldsymbol{\Phi}_i^e$ is the nodal displacement mode vector of the ith beam element in the local coordinate system.

In the ith beam element, the amount of nodal displacement mode information contained in the strain mode vector can be obtained from the expression of transformation matrix $\mathbf{B}_i$, and each row of $\mathbf{B}_i$ is corresponding to a candidate strain gauge location

$$\begin{aligned}\mathbf{B}_{ij} &= \frac{1}{l^3}\times \\ &[-l^2, 6yl-12xy, 6zl-12xz, 0, 6xzl-4zl^2, 4yl^2-6xyl, \\ &\ l^2, 12xy-6yl, 12xz-6zl, \ 0, 6xzl-2zl^2, 2yl^2-6xyl \ ]\end{aligned} \tag{22}$$

where $\mathbf{B}_{ij}$ is the jth row of $\mathbf{B}_i$; l is the length of the beam element and x, y and z are the coordinates of the strain gauge location in the local coordinate system. Each row of $\mathbf{B}_i$ has the same form and is only affected by the specific location of each candidate strain gauge location. From Eq. (22), the 12 variables in $\mathbf{B}_{ij}$ correspond to the 12 degrees of freedom of the two nodes of the ith beam element. More specifically, the 1st, 2nd and 3rd variables denote the three degrees of freedom of translation modes of the beginning node; the 4th, 5th and 6th variables denote the three degrees of rotation modes of the beginning node. Similarly, the 7th, 8th and 9th variables denote the three degrees of freedom of translation modes of the ending node; the 10th, 11th and 12th variables denote the three degrees of rotation modes of the ending node. When some displacement modes of estimated locations need to be estimated based on the strain modes obtained from the selected strain gauge locations, the locations of the strain gauges should contain as much information regarding the displacement modes as possible. Here, the estimated locations correspond to the accelerometers; thus, the translation modes must be estimated. The 1st to 3rd and the 7th to 9th variables of $\mathbf{B}_{ij}$ correspond to the translation modes, and the values of the six variables are important to the estimation quality. If the values of these variables are zero, no translation mode information can be contained in the strain modes. In the existing papers, strain gauges are often placed at the midpoint of each beam element because the largest deflection often occurs at the midpoint of a beam. However, from the point of view of this paper, when $x = 0.5l$, the 2nd, 3rd, 8th and 9th variables of $\mathbf{B}_{ij}$ all equal zero, which means that the selected strain gauges placed at these locations contain no translation mode information. Thus, if the translation modes must be estimated based on the strain modes, placing strain gauges at the midpoints of beam elements is unreasonable. It is interesting to note that when performing translation mode estimation, different candidate locations of the strain gauges can greatly affect the estimation result.

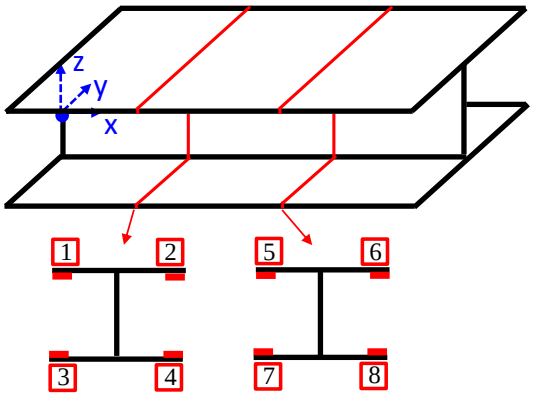

Fig. 6 Candidate strain gauge locations on each beam element in the local coordinate system

Each accelerometer location corresponds to three rows of the displacement mode shape matrix, which are the translation mode shapes. Thus, in this paper, the translation modes need to be estimated, and the rotation modes do not need to be estimated, which means that when selecting initial candidate strain gauge locations, as much translation mode information as possible should be contained, and rotation modes should be avoided to reduce the estimation error and computational effort. Consequently, the initial candidate strain gauge locations on each beam element are at 1/3 and 2/3 the longitudinal length of the beam, and the strain gauges must be placed on the flange of the beam element at the same time to ensure that the variables in $\mathbf{B}_{ij}$ corresponding to the translation modes are nonzero. As shown in Fig. 6, on each beam element, the red lines represent the cross sections at 1/3 and 2/3 the longitudinal length of the beam element, while the 8 red solid rectangles represent the strain gauge locations, with the numbers from 1 to 8 used to mark the specific locations.

3.3 Estimation results

3.3.1 Decreasing some initial accelerometer locations in order

Here, the last 3 added locations of the initial accelerometer locations are deleted from the initial accelerometer locations. Fig. 7 shows the locations of the 5 remaining accelerometers and the 3 deleted accelerometers, where the red solid circles denote the remaining accelerometer locations, while the red diamonds denote the estimated locations. To estimate the translation modes of the 3 estimated locations, 9 strain gauges are needed here to ensure that when estimating the translation modes, the number of selected strain gauges is greater than or equal to the number of rows of the translation modes. Then, the MAC is used to evaluate the displacement mode information from the sensor placement, and the change of the value of the maximum off-diagonal MAC term is used as a criterion to evaluate the performance of the proposed sensor placement.

Fig. 8 demonstrates the locations of the obtained final sensor placement, which consists of five accelerometers and

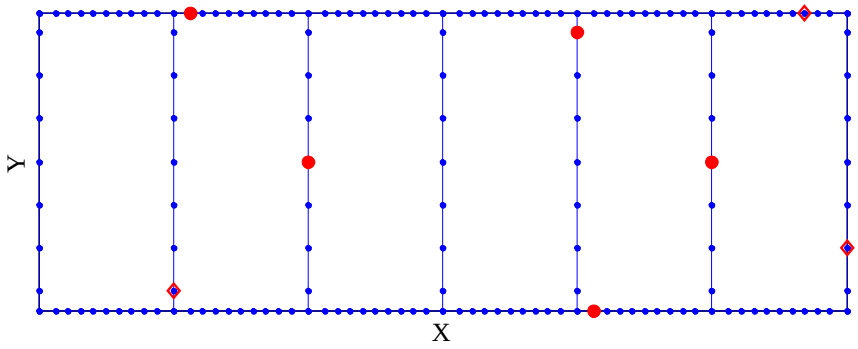

Fig. 7 Five remaining accelerometer locations and 3 estimated locations

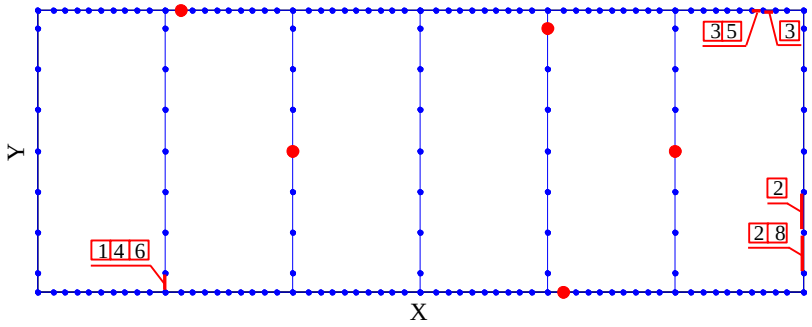

Fig. 8 Final sensor placements of 5 accelerometers and 9 strain gauges

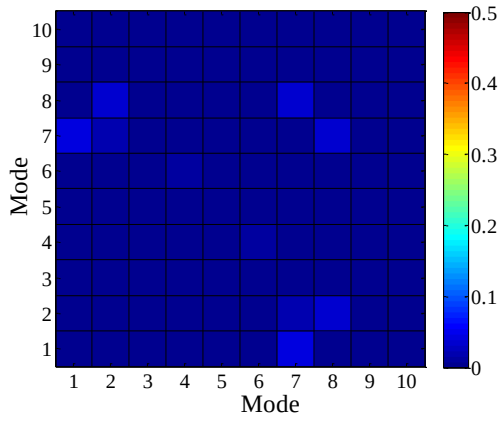

(a) 8 initial accelerometers

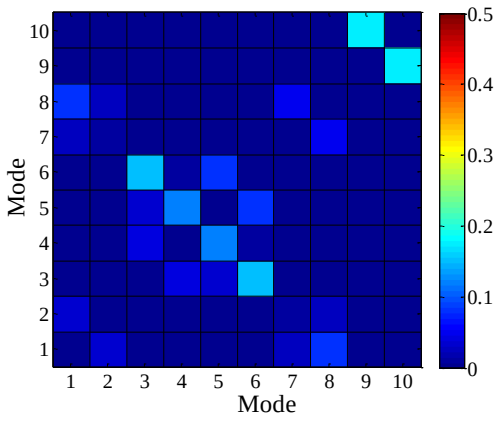

(b) 5 remaining accelerometers

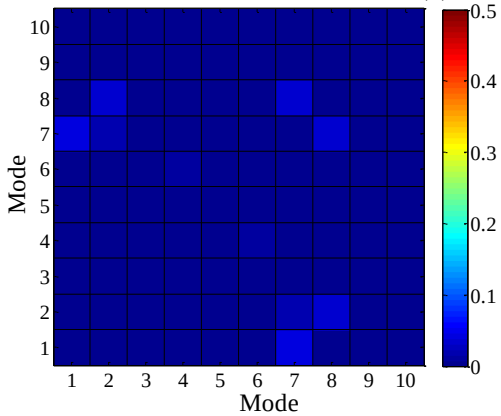

(c) final sensor placement of 5 accelerometers and 9 strain gauges

Fig. 9 Off-diagonal MAC values of different sensor placements

Table 1 Values of maximum off-diagonal MAC terms of different selected sensor locations

Different sensor locations	8 initial locations	5 remaining locations	Final locations
Maximum off-diagonal value	0.0448	0.1739	0.0451

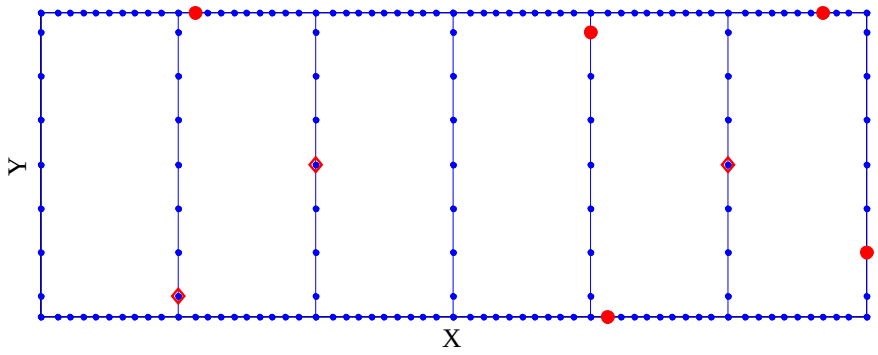

Fig. 10 Five remaining accelerometer locations and 3 estimated locations

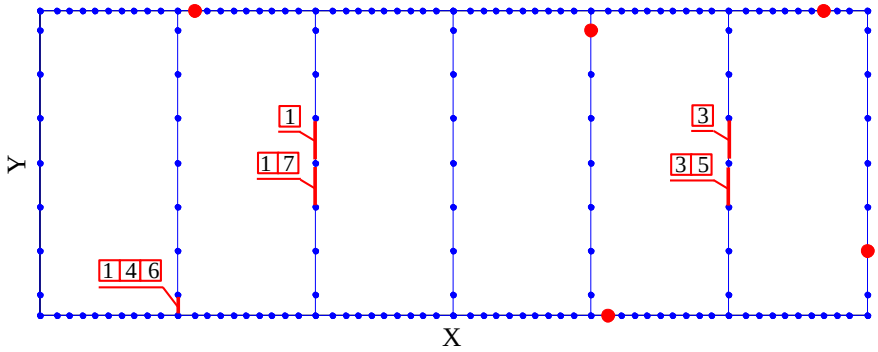

Fig. 11 Final sensor placements of 5 accelerometers and 9 strain gauges

nine strain gauges. It can be seen in Fig .8 that the red solid circles represent the selected accelerometer locations and the red lines are the beams on which strain gauges should be placed; the specific locations of the strain gauges can be found in Fig. 6 according to the numbers in the comment boxes. The displacement modes of the final sensor locations consist of the displacement modes of the 5 accelerometer locations and the displacement modes estimated based on the strain modes of the 9 strain gauges. Fig. 9 shows the values of off-diagonal MAC terms of different selected sensor locations, and the diagonal terms are defined as zero. The values of maximum off-diagonal MAC terms of different selected sensor locations are listed in Table 1. Comparing Fig. 9(a) with Fig. 9(b), an increase in MAC values can be observed, and the increase is not very obvious because of the feature of the sequential algorithm used for selecting accelerometer locations, i.e., that the last three locations do not cause a huge decrease in the MAC values. Comparing Fig. 9(b) with Fig. 9(c), the MAC values decrease, which indicates that the strain gauges help improve the performance of the sensor placement. Comparing Fig. 9(c) with Fig. 9(a), the MAC values are similar, indicating that the obtained multitype sensor placement achieves a good performance under the MAC when compared to the initial accelerometers. In this situation, the proposed sensor placement method is effective in helping to obtain more accurate displacement mode information of the structure under MAC.

3.3.2 Decreasing the number of initial accelerometers randomly

To compare with the case of deleting sensors in order, 3 accelerometers from the initial accelerometer locations are randomly deleted. Fig. 10 demonstrates the locations of the 5 remaining accelerometers and the 3 deleted accelerometers, in which the red solid circles represent the remaining accelerometer locations and the red diamonds are the estimated locations. To estimate the translation modes of the 3 estimated locations, 9 strain gauges are needed here to ensure that when estimating the translation modes, the number of selected strain gauges is greater than or equal to the number of rows of the translation modes. Similarly, the MAC is used to evaluate the displacement mode information from the sensor placement, and the change of the value of the maximum off-diagonal MAC term is used as a criterion to evaluate the performance of the proposed sensor placement.

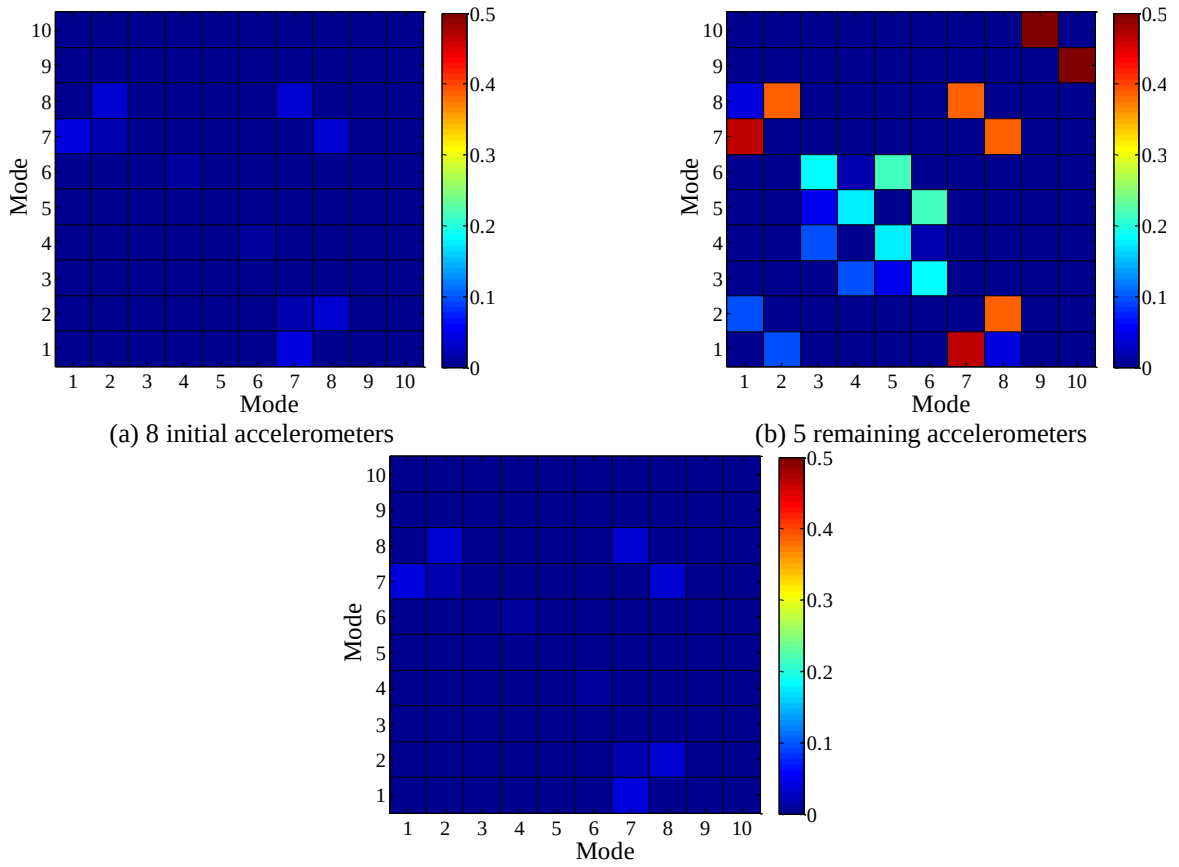

(a) 8 initial accelerometers

(b) 5 remaining accelerometers

(c) final sensor placement of 5 accelerometers and 9 strain gauges

Fig. 12 Off-diagonal MAC values of different sensor placements

Table 2 Values of maximum off-diagonal MAC terms of different selected sensor locations

Different sensor locations	8 initial locations	5 remaining locations	Final locations
Maximum off-diagonal value	0.0448	0.4624	0.0454

Fig. 11 gives the locations of the final sensor placement, consisting of 5 accelerometers and 9 strain gauges, in which the red solid circles represent the accelerometer locations and the red lines are the beams on which the strain gauges are placed; the specific locations of the strain gauges can be found in Fig. 6 according to the numbers in the comment boxes. The displacement modes of the final sensor locations consist of the displacement modes of the 5 accelerometer locations and the displacement modes estimated based on the strain modes of the 9 strain gauges. Fig. 12 demonstrates the values of the off-diagonal MAC terms of different selected sensor locations, and the diagonal terms are also defined as zero. Table 2 lists the values of the maximum off-diagonal MAC terms of different selected sensor locations. Comparing Fig. 12(a) with Fig. 12(b), the value of the maximum off-diagonal MAC term obviously increases because the 3 sensors are randomly deleted from the initial accelerometers and the remaining sensor locations cannot satisfy the MAC well. Comparing Fig. 12(c) with Fig. 12(b), the value of the maximum off-diagonal MAC term obviously decreases, which indicates that the strain gauges help much in improving the performance of the sensor placement. Comparing Fig. 12(c) with Fig. 12(a), the MAC values are similar, which demonstrates that the obtained multitype sensor placement performs well under the MAC when compared to the initial accelerometers. In this situation, the proposed sensor placement method is effective in helping to obtain more accurate displacement mode information of the structure under MAC.

To see the effectiveness of the proposed estimation theory, the estimation of displacement modes of the estimated locations is performed. In the above two cases, as shown in Figs. 7 and 10, there are five different estimated locations. According to Eqs. (13) and (16), a normal distribution noise is added to the mode shape obtained from the FE model, the noise level σ_i is determined as the 5% and 10% of the maximum value in the ith column of the mode shape matrix. The estimation results about displacement modes of first several orders are shown in Figs. 13 and 14. As shown in Figs. 13 and 14, the red lines is the error bar of the estimated result, which corresponds to the 95% confidence interval. When noise level is 5%, the maximum absolute estimation error is below 3%; when

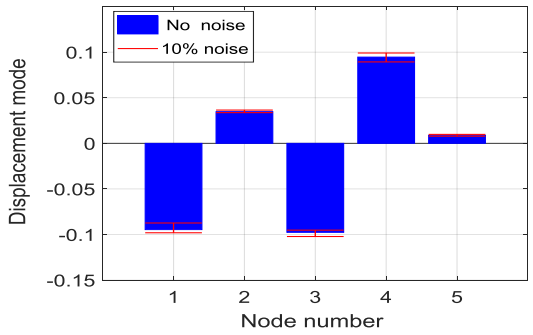

(a) 1st mode shape in y direction

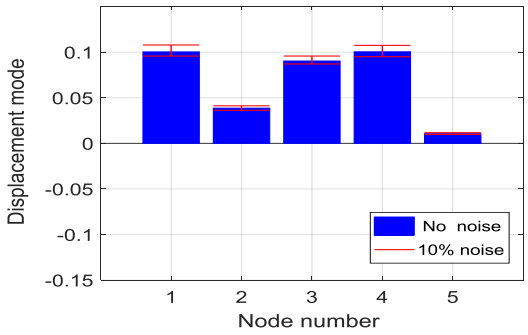

(b) 2nd mode shape in y direction

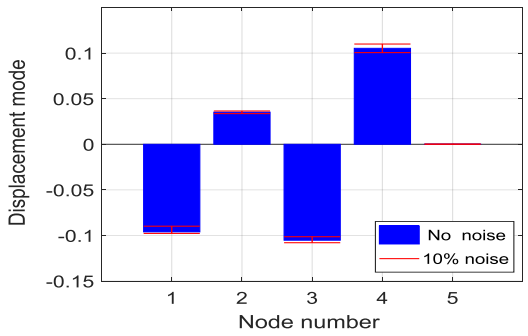

(c) 3rd mode shape in z direction

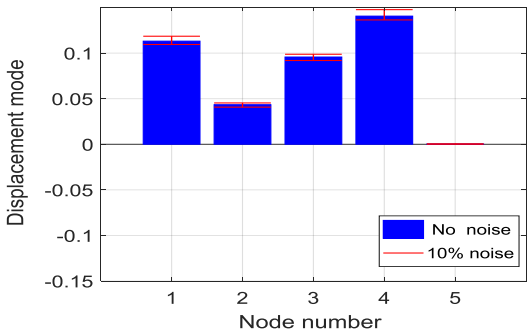

(d) 4th mode shape in z direction

Fig. 13 Estimated displacement modes on the 5 nodes under 10% noise

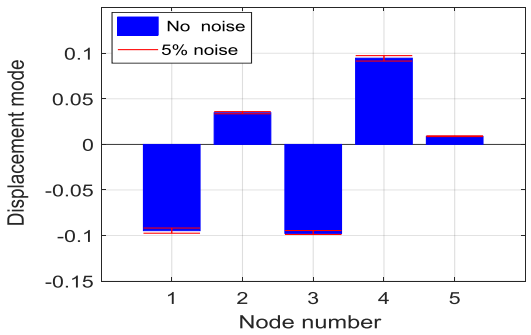

(a) 1st mode shape in y direction

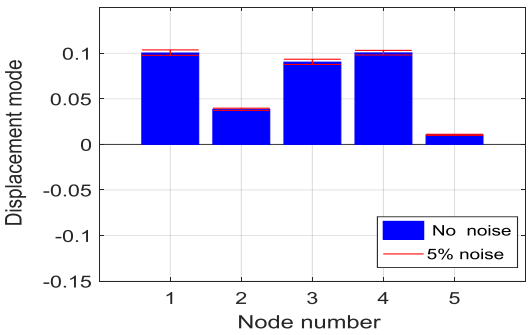

(b) 2nd mode shape in y direction

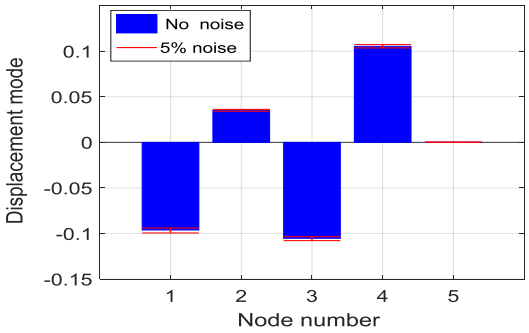

(c) 3rd mode shape in z direction

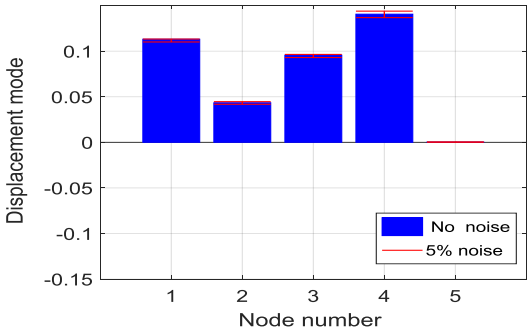

(d) 4th mode shape in z direction

Fig. 14 Estimated displacement modes on the 5 nodes under 10% noise

noise level is 10%, the maximum absolute estimation error is below 6%. Considering the centralization of normal distribution，the accuracy of the estimation result of the displacement modes is acceptable. In addition, the changes in mode shapes caused by the model error are usually small, which means the noise level is small. Thus, the proposed method for modal estimation of structures is meaningful and effective.

Furthermore, instead of deleting locations from the initial accelerometer locations, if more translation mode

information is needed, the locations added to the initial accelerometer locations according to Fig. 5 are defined as estimated locations; then, strain gauge locations are selected to estimate the translation modes of the estimated locations. The selection process is similar to the method mentioned above.

4. Conclusions

In this paper, the problem of the comprehensive placement of strain gauges and triaxial accelerometers for obtaining structural displacement mode information is solved by using the proposed modal estimation theory. A bridge benchmark structure is used here for a numerical investigation. Some conclusions are as follows:

- A modal estimation theory using the relationship between the strain mode and displacement mode is proposed. Through this theory, the displacement modes of the estimated locations without accelerometers can be estimated by the strain modes obtained from some selected strain gauge measurements. The trace value of the covariance matrix of the estimated displacement mode vector is used to represent the uncertainty of the estimation. The strain gauge locations corresponding to the smallest trace value are final selected for obtaining more accurate displacement mode information.
- The MAC and the redundancy information are utilized together for guiding the initial accelerometer location selection, in which the distinguishability and small redundancies of the obtained displacement modes are guaranteed. In this paper, decreasing the initial accelerometer locations, which are defined as the estimated locations, in order or randomly can simulate the practical situation of decreasing the selected accelerometer locations well.
- When performing displacement mode estimation, the candidate strain gauge positions should be determined according to the contained displacement mode information. In the existing studies about optimal sensor placement problem involving the strain gauges, strain sensors are often simply placed on the midpoints of each beam elements without explanation. In this paper, the amount of the displacement mode information contained in the strain mode locations is defined by the elements in the transformation matrix. In the used bridge benchmark structure, the candidate strain gauge locations need to contain as much displacement mode information as possible without being at the midpoints.
- The MAC is used to evaluate the displacement mode information obtained from the sensor placement. Compared to the initial accelerometer placement and the remaining accelerometer placement, the obtained multitype sensor placement has similar and smaller MAC values, which demonstrates the good performance of the proposed multitype sensor placement method under the MAC. In addition, the estimation of displacement modes of the estimated locations is performed. The accuracy of the estimation result of the displacement modes is acceptable, which verifies the effectiveness of the proposed method for modal estimation of structures.

Acknowledgments

This research work was jointly supported by the National Natural Science Foundation of China (Grant No. 51625802, 51478081), and the 973 Program (Grant No. 2015CB060000).

References

Beck, J.L. and Katafygiotis, L.S. (1998), "Updating models and their uncertainties. I: Bayesian statistical framework", *J. Eng. Mech.-ASCE*, **124**(4), 455-461.

Catbas, F.N., Gul, M., and Burkett, J.L. (2008). "Damage assessment using flexibility and flexibility-based curvature for structural health monitoring", *Smart Mater. Struct.*, **17**(1), 015024.

Carne, T.G. and Dohrmann, C.R. (1995), "A modal test design strategy for model correlation", *Proceedings-SPIE the International Society for Optical Engineering*, Nashville, USA, Feb.

Chang, M. and Pakzad, S.N. (2014), "Optimal sensor placement for modal identification of bridge systems considering number of sensing nodes", *J. Bridge Eng.-ASCE*, **19**(6), 04014019.

Heo, G., Wang, M.L. and Satpathi, D. (1997), "Optimal transducer placement for health monitoring of long span bridge", *Soil Dyn. Earthq. Eng.*, **16**(7), 495-502.

Huang, H.B., Yi, T.H. and Li, H.N. (2017), "Bayesian combination of weighted principal component analysis for diagnosing sensor faults in structural monitoring systems", *J. Eng. Mech.-ASCE*, **143**(9), 04017088.

Johnson, R.A. and Wichern, D.W. (2002), *Applied multivariate statistical analysis*, Prentice Hall, London, UK.

Kammer, D.C. (1991), "Sensor placement for on-orbit modal identification and correlation of large space structures", *J. Guid. Control Dynam.*, **14**(2), 251-259.

Kammer, D.C. and Tinker, M.L. (2004), "Optimal placement of triaxial accelerometers for modal vibration tests", *Mech. Syst. Signal Pr.*, **18**(1), 29-41.

Li, D.S., Li, H.N. and Fritzen, C.P. (2007), "The connection between effective independence and modal kinetic energy methods for sensor placement", *J. Sound Vib.*, **305**(4), 945-955.

Li, J. and Hao, H. (2016), "A review of recent research advances on structural health monitoring in Western Australia", *Struct. Monit. Maint.*, **3**(1), 33-49.

Li, J., Hao, H. and Chen, Z.W. (2017), "Damage identification and optimal sensor placement for structures under unknown traffic-

induced vibrations", *J. Aerosp. Eng.- ASCE*, **30**(2), B4015001.
Papadimitriou, C., Beck, J.L. and Au, S.K. (2000), "Entropy-based optimal sensor location for structural model updating", *J. Vib. Control*, **6**(5), 781-800.
Papadimitriou, C. and Lombaert, G. (2012), "The effect of prediction error correlation on optimal sensor placement in structural dynamics", *Mech. Syst. Signal Pr.*, **28**(2), 105-127.
Papadopoulos, M. and Ephrahim, G. (1998), "Sensor placement methodologies for dynamic testing", *AIAA J.*, **36**(2), 256-263.
Penny, J.E.T., Friswell, M.I. and Garvey, S.D. (1994), "Automatic choice of measurement locations for dynamic testing", *AIAA J.*, **32**(2), 407-414.
Ren, L., Yuan, C.L., Li, H.N. and Yi, T.H. (2016), "Structural Health Monitoring System Developed for Dalian Stadium", *Int. J. Struct. Stab. Dy.*, **16**(4), 1640018.
Shi, Z.Y., Law, S.S. and Zhang, L.M. (2000), "Optimum sensor placement for structural damage detection", *J. Eng. Mech.-ASCE*, **126**(11), 1173-1179.
Stephan, C. (2012), "Sensor placement for modal identification", *Mech. Syst. Signal Pr.*, **27**, 461-470.
Udwadia, F.E. (1994), "Methodology for optimum sensor locations for parameter identification in dynamic systems", *J. Eng. Mech.-ASCE*, **120**(2), 368-390.
Worden, K. and Burrows, A. P. (2001), "Optimal sensor placement for fault detection", *Eng. Struct.*, **23**(8), 885-901.
Yam, L.Y., Leung, T.P., Li, D.B. and Xue, K.Z. (1996), "Theoretical and experimental study of modal strain analysis", *J. Sound Vib.*, **191**(2), 251-260.
Yi, T.H., Li, H.N. and Gu, M. (2012a), "Sensor placement for structural health monitoring of Canton Tower", *Smart Struct. Syst.*, **10**(4-5), 313-329.
Yi, T.H., Li, H.N. and Zhang, X.D. (2012b), "Sensor placement on Canton Tower for health monitoring using asynchronous-climb monkey algorithm", *Smart Mater. Struct.*, **21**(12), 125023.
Yi, T.H., Li, H.N. and Wang, C.W. (2015a), "Multiaxial sensor placement optimization in structural health monitoring using distributed wolf algorithm", *Struct. Control. Health.*, **23**(4), 719-734.
Yi, T.H., Zhou, G.D., Li, H.N. and Zhang, X.D. (2015b), "Optimal sensor placement for health monitoring of high-rise structure based on collaborative-climb monkey algorithm", *Struct. Eng. Mech.*, **54**(2), 305-317.
Yuen, K.V. and Kuok, S.C. (2015), "Efficient Bayesian sensor placement algorithm for structural identification: a general approach for multi-type sensory systems", *Earthq. Eng. Struct. D.*, **44**(5), 757-774.
Zhang, X.H, Xu, Y.L., Zhu, S. and Zhan, S. (2014), "Dual-type sensor placement for multi-scale response reconstruction", *Mechatronics*, **24**(4), 376-384.
Zhang, C.D. and Xu, Y.L. (2016), "Optimal multi-type sensor placement for response and excitation reconstruction", *J. Sound Vib.*, **360**, 112-128.